to the toe 60 min after the intravenous injection of ^{18}F-FDG (5 MBq/kg), 20 min after the injection of ^{11}C-MET (370 MBq), or 40 min after the injection of ^{11}C-4DST (370 MBq). The SUV consistency for these two PET/CT scanners was validated using a phantom study. Low-dose CT was performed first for attenuation correction and image fusion. Emission images were acquired in a three-dimensional mode for 2 min per bed position using both PET/CT scanners. The PET/CT data were reconstructed using a Gaussian filter with an ordered subset expectation maximization algorithm (3 iterations, 8 subsets for Biograph 16, 3 and 16 subsets for Discovery PET/CT 600, according to the manufacturers' recommendations).

The radiation exposure from ^{11}C-labeled radiopharmaceuticals is much lower than that from ^{18}F-labeled radiopharmaceuticals. The estimated effective dose for ^{11}C-4DST is 1.6 mSv [19], that for ^{11}C-MET is 2.1 mSv, that for ^{18}F-FDG is 7 mSv [22], and that for low-dose CT is 1.4–3.5 mSv. Therefore, the total effective dose delivered during all the PET/CT examinations was about 14.9–21.2 mSv. We felt that the radiation exposure from the PET/CT examinations performed in the present study was acceptable when their impact on the therapeutic strategy was considered.

PET data analysis

Xeleris (GE Healthcare) and e-Soft (Siemens) workstations were used for image analysis. The physiological uptake of ^{11}C-MET is seen in the gastrointestinal tract, liver, pancreas, urinary tract, and salivary glands, as reported by Nishizawa et al. [15]. A high physiological ^{11}C-4DST uptake is observed in the salivary glands, liver, spleen, kidneys, bladder, and bone marrow. In contrast, the brain, lungs, myocardium, muscle, and blood pool exhibit a low physiological ^{11}C-4DST uptake [20]. The SUVmax of ^{11}C-4DST in the normal bone marrow is higher than that of ^{18}F-FDG (lumbar vertebrae 2–4, ilium, proximal humeri, and proximal femurs), and the SUVmax of ^{11}C-MET falls between these two values. Based on this normal background, the active accumulations of ^{18}F-FDG, ^{11}C-MET, and ^{11}C-4DST in the bone marrow lesions were evaluated.

Two experienced nuclear medicine physicians visually evaluated all the PET/CT scans for tracer accumulation in the lesions (positive, equivocal, or negative); the maximum standardized uptake value (SUVmax) was also recorded for each lesion. If the results of the two physicians differed, the physicians discussed the findings and reached a consensus. To evaluate the bone marrow lesions on the ^{11}C-MET and ^{11}C-4DST PET/CT images, the scale and window of the monitor display for these PET/CT images had to be adjusted so that the pathological uptake could be visualized with a better contrast against the high physiological uptake in the normal bone marrow. Before the start of this study, the physicians underwent training that included images from more than ten patients who had non-MM without bone diseases, since Nakamoto et al. [23] reported that suspicious lesions, including those in the bone marrow, could be clearly depicted using a proper display window and level in their ^{11}C-MET PET/CT study. Focal accumulation that was higher than the background was regarded as being positive, no accumulation compared with the

Table 2 Correlation between cytology and PET/CT findings

Pt No	Plasma cell (%)	FDG	MET	4DST
1	84	○	○	○
2	81.5	○	○	○
3	71.2	○	○	○
4	67.4	○	○	○
5	58.8	○	○	○
6	45.4	×	○	○
7	43.6	△	○	○
8	36	△	○	○
9	30.4	×	○	○
10	21.4	×	×	×
11	21	×	×	○
12	17	×	○	○
13	12	△	△	○
14	10.6	×	○	○
15	10	△	△	○
16	8.8	×	×	×
17	8.5	×	×	×
18	8.2	×	×	×
19	7.8	×	×	×
20	4.4	△	○	○
21	2.6	×	×	×
22	1.6	×	×	×
23	1.2	○	○	○
24	1	×	×	×
25	1	×	×	×
26	0.8	×	×	×
27	0.6	×	×	×
28	0.6	×	×	△
29	0.4	×	×	×
30	0.4	△	△	△
31	0.4	×	×	×
32	0.4	×	×	×
33	0.3	×	×	×
34	0.2	×	×	×
35	0	△	○	○
36	0	△	△	△

Note 10 % of the plasma cells in the cytology specimen is the threshold for active myeloma

PET/CT findings: positive ○, equivocal △, negative ×

background was regarded as being negative, and accumulation with the same level as the background was regarded as being equivocal.

Focal lytic lesions

In 24 patients (before receiving therapy, 6 patients; after receiving therapy, 18 patients), a total of 55 focal lytic lesions (before receiving therapy, 10 lesions, after receiving therapy, 45 lesions) were detected using CT when PET/CT was performed, but no diffuse lesions were detected. The sizes of the 55 focal lytic lesions were 23.7 ± 13.8 mm (range 6–70 mm), which was sufficiently large to be evaluated using low-dose CT and PET/CT.

Comparison to marrow plasma cells cytology

The percentages of marrow plasma cells in the posterior iliac crests were calculated using bone marrow aspiration smears in 36 patients (Table 2) within 1 week before or after the three PET/CT studies. Eleven of the patients were also included in the first study. According to the criteria of the International Myeloma Working Group, a bone marrow clonal cell percentage of more than 10 % is regarded as a positive pathology for active myeloma and should be regarded as the gold standard for diagnosis [24].

We evaluated the accumulation of ^{18}F-FDG, ^{11}C-MET, and ^{11}C-4DST in the posterior iliac crests from where the bone marrow samples were obtained. The tracer accumulation was evaluated visually as positive, equivocal, or negative uptake. Even if abnormal accumulation was visible in lesions other than the posterior iliac crests, a positive-uptake evaluation was not made. Also, when an artifact from the bone marrow puncture was observed, the artifact was carefully excluded from the evaluation. Then, we compared the sensitivity, specificity, positive predictive value, negative predictive value, and accuracy rate of PET/CT using each of the three tracers.

Statistical analysis

The significance of the differences in the accumulation of the three tracers was determined using the area under the curve with a receiver operating characteristic (ROC) analysis. The significance of the differences between bone marrow aspiration and the accumulation of each of the three tracers was determined using the Fisher exact test. *P* values less than 0.05 were considered to be statistically significant.

Results

Focal lytic lesions

Both before and after therapy, the number of equivocal lesions observed using ^{18}F-FDG was larger than that observed using ^{11}C-MET or ^{11}C-4DST. For ^{11}C-4DST, ^{11}C-MET, and ^{18}F-FDG, the highest SUVmax values were observed, in order, for positive, equivocal and negative lesions (Table 3). Among the patients who were examined after therapy, in particular, ^{11}C-MET or ^{11}C-4DST was capable of detecting positive lesions more frequently than ^{18}F-FDG.

^{18}F-FDG was rarely able to detect skull lesions because of the high physiological accumulation in the brain, whereas ^{11}C-MET and ^{11}C-4DST were capable of clearly detecting skull lesions because of their low accumulation in the brain (Fig. 2). A typical MM patient with multiple active lesions is sh own in Fig. 3. ^{11}C-MET and ^{11}C-4DST detected positive lesions, whereas ^{18}F-FDG detected an equivocal lesion. The lesion was positive when evaluated using MRI and negative when evaluated using CT (Fig. 4).

Table 3 Accumulation of ^{18}F-FDG, ^{11}C-MET, and ^{11}C-4DST in lytic lesions on CT

	Number of lesions				SUVmax		
	Positive	Equivocal	Negative	Total	Positive	Equivocal	Negative
Patients examined before therapy							
^{18}F-FDG	6	2	2	10	4.00 ± 1.63	1.98	1.55
^{11}C-MET	10	0	0	10	5.74 ± 2.15	–	–
^{11}C-4DST	8	0	2	10	15.8 ± 9.79	–	3.5
Patients examined after therapy							
^{18}F-FDG	27	8	10	45	3.20 ± 1.70	2.05 ± 0.28	1.55 ± 0.41
^{11}C-MET	39	3	13	45	5.01 ± 2.40	3.89 ± 1.87	2.19 ± 1.28
^{11}C-4DST	32	1	12	45	6.44 ± 3.07	4.25	3.39 ± 3.29
Total patients							
^{18}F-FDG	33	10	12	55	3.35 ± 1.70	2.03 ± 0.26	1.54 ± 0.38
^{11}C-MET	39	3	13	55	5.19 ± 2.40	3.89 ± 1.87	2.19 ± 1.28
^{11}C-4DST	40	1	14	55	8.30 ± 6.24	4.25	3.40 ± 3.02

Data are the mean ± SD

SUVmax maximum standardized uptake values

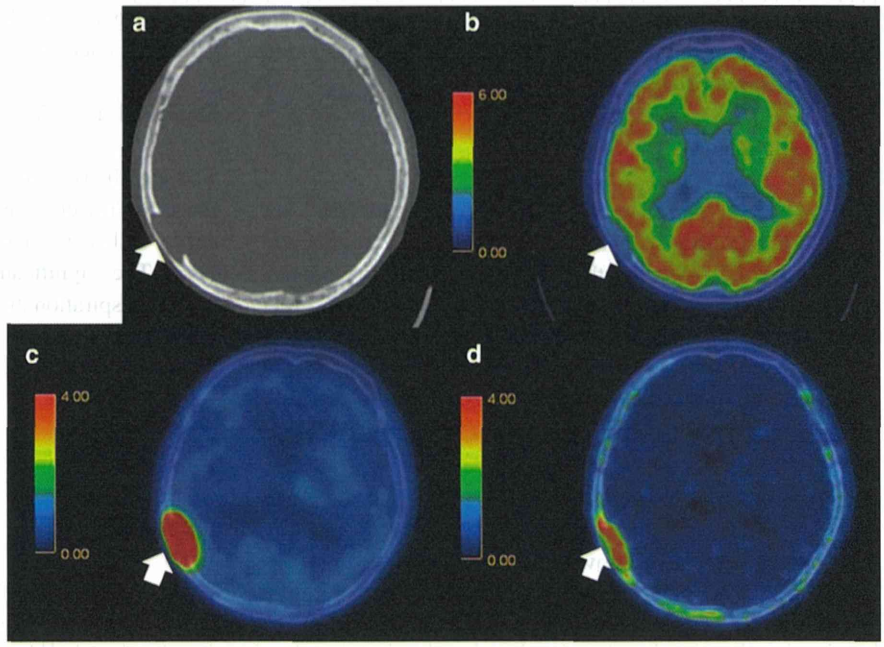

Fig. 2 Fusion images of **a** CT, **b** ^{18}F-FDG, **c** ^{11}C-MET, and **d** ^{11}C-4DST obtained in a 79-year-old woman with multiple myeloma (IgG-κ). The *arrow* shows an osteolytic lesion. ^{11}C-MET PET/CT and ^{11}C-4DST PET/CT detected activity in the skull lesion, whereas ^{18}F-FDG PET/CT could not detect any activity because of normal brain accumulation

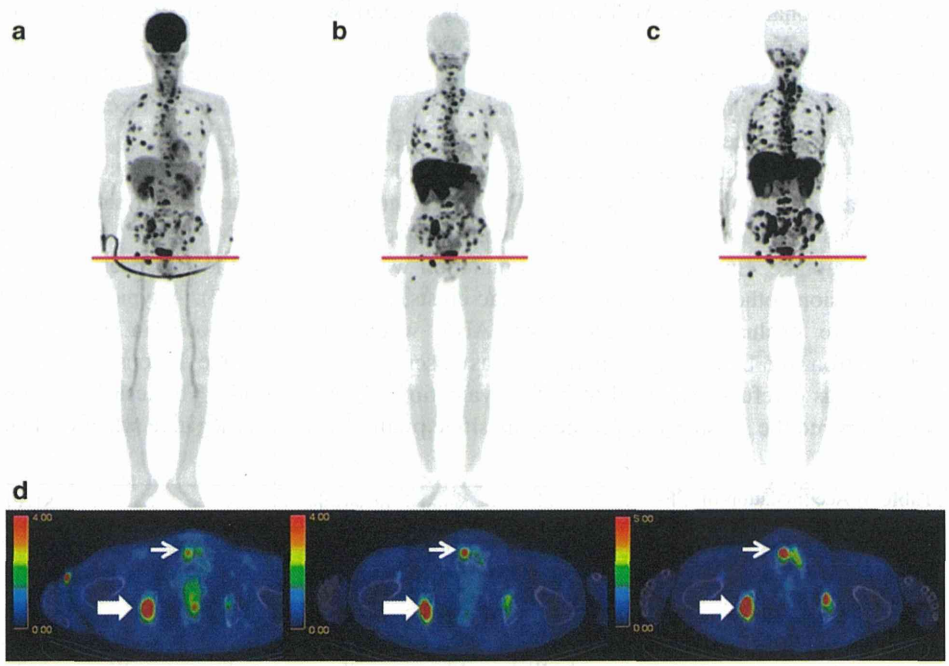

Fig. 3 Maximum intensity projection images and fusion images. **a** ^{18}F-FDG, **b** ^{11}C-MET, and **c** ^{11}C-4DST PET images obtained in a 63-year-old man (Patient 1) with MM (IgA-κ). Numerous active lesions are visible in the three maximum intensity projection images. The fusion images are for the cross-section at the level of the *red lines* (**d**). The lesion in the right ischium (*bold arrow*) was positive on all three PET scans. However, the lesion in the right pubis (*narrow arrow*) was only positive on the ^{11}C-MET PET and ^{11}C-4DST PET scans and was equivocal on the ^{18}F-FDG PET scan (color figure online)

Comparison to marrow plasma cells cytology

A Fisher exact test demonstrated a significant correlation between positive uptake on the PET/CT scans and a positive pathology of the bone marrow plasma cells. The *P* values of ^{11}C-MET and ^{11}C-4DST were lower than that of ^{18}F-FDG. The diagnostic potentials of the three tracers are as described below. ^{11}C-4DST showed the highest sensitivity. The specificity of the three tracers was comparable (Table 4). The ROC analysis showed statistically significant differences between ^{18}F-FDG and ^{11}C-MET and between ^{18}F-FDG and ^{11}C-4DST (Table 5). The area under the ROC curves for ^{11}C-MET and ^{11}C-4DST were greater than that for ^{18}F-FDG. The other three indices for ^{11}C-MET and ^{11}C-4DST were larger than those for ^{18}F-FDG. But no statistically significant differences in the positive

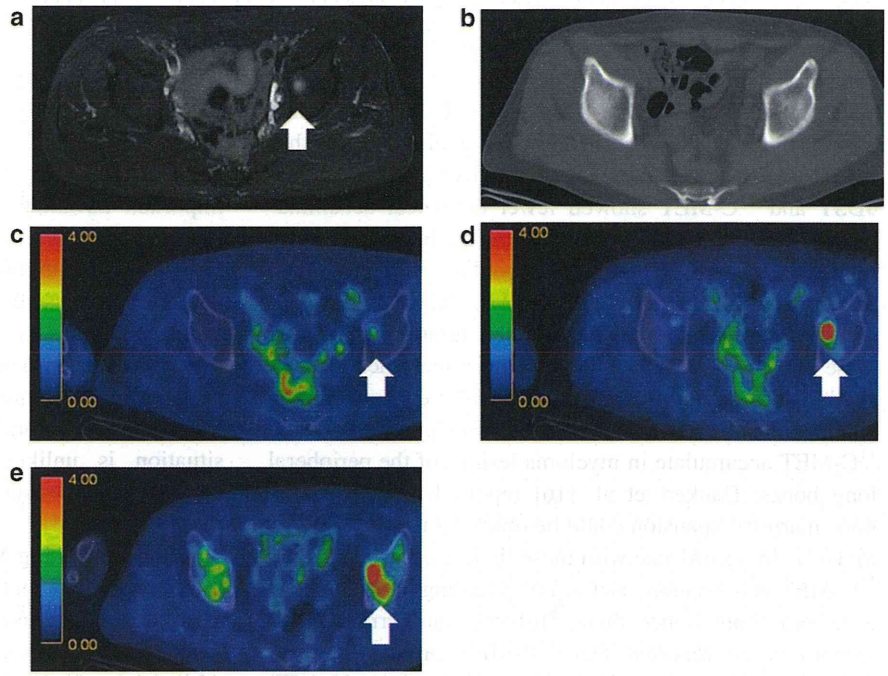

Fig. 4 **a** CT and **b** MRI fusion images of **c** ^{18}F-FDG PET/CT, **d** ^{11}C-MET PET/CT, and **e** ^{11}C-4DST PET/CT obtained in a 63-year-old man. The acetabular lesion was positive on the MRI, ^{11}C-MET PET/CT, and ^{11}C-4DST PET/CT images, equivocal on the ^{18}F-FDG PET scans, and negative on the CT images

Table 4 Contingency correlating PET/CT positivity with disease activity according to bone marrow aspiration and diagnostic results of PET/CT using each of the three tracers

PET/CT finding	Bone marrow aspiration		*P* value
Fisher exact test	Positive	Negative	
^{18}F-FDG			
Positive	9	5	0.03
Negative	6	16	
^{11}C-MET			
Positive	13	5	0.0005
Negative	2	16	
^{11}C-4DST			
Positive	14	6	0.0001
Negative	1	15	

	^{18}F-FDG	^{11}C-MET	^{11}C-4DST
Sensitivity	60.0	86.7	93.3
Specificity	76.1	76.1	71.4
Positive predictive value	64.3	72.2	70.0
Negative predictive value	72.7	88.9	93.7
Accuracy rate	69.4	80.6	80.6

A Fisher exact test demonstrated a significant correlation between positive uptake on the PET/CT scans and a positive pathology of the bone marrow plasma cells

predictive value, negative predictive value, and accuracy rate were observed among the three tracers when examined using a Chi square test ($P > 0.05$).

Table 5 Area under the receiver operating characteristic curve

Area	Difference	
^{18}F-FDG		
0.681 (95 % CI, 0.522–0.840)		
^{11}C-MET		
0.814 (95 % CI, 0.685–0.943)	vs. ^{18}F-FDG	
	$P = 0.02$	
^{11}C-4DST		
0.824 (95 % CI, 0.705–0.942)	vs. ^{18}F-FDG	vs. ^{11}C-MET
	$P = 0.03$	$P = 0.81$

CI confidence interval

In patients with more than 58 % plasma cells, all the PET/CT data showed a positive uptake. However, in patients with 10–30 % plasma cells, ^{11}C-MET and ^{11}C-4DST detected larger numbers of positive-uptake lesions than ^{18}F-FDG (Table 2).

All three PET/CT scans were negative for all three MGUS patients. Extramedullary lesions were not evaluated in the present study.

Discussion

We demonstrated the usefulness of ^{11}C-4DST and ^{11}C-MET PET/CT imaging, compared with ^{18}F-FDG PET/CT imaging, in patients with MM. ^{11}C-4DST and ^{11}C-MET provided clearer findings than ^{18}F-FDG for lytic lesions

visible using CT. Furthermore, ^{11}C-4DST and ^{11}C-MET had higher diagnostic accuracies than ^{18}F-FDG, when compared using iliac crest biopsy data.

In the first study, ^{11}C-4DST and ^{11}C-MET provided clearer findings than ^{18}F-FDG when evaluating whether lytic lesions detected using CT were active or inactive. ^{11}C-4DST and ^{11}C-MET showed fewer equivocal accumulations than ^{18}F-FDG. Osteolytic lesions are more commonly found in the axial skeleton, skull, shoulder girdle, proximal humeri, ribs, and proximal femurs [25]. ^{11}C-4DST and ^{11}C-MET were useful for evaluating the tumor activities of these lesions. As shown in Fig. 2, the disease activities of skull lesions can typically be successfully evaluated using ^{11}C-4DST and ^{11}C-MET, but not ^{18}F-FDG. ^{11}C-4DST and ^{11}C-MET accumulate in myeloma lesions of the peripheral long bones. Dankerl et al. [16] reported that peripheral bone marrow expansion could be observed using ^{11}C-MET PET/CT. In accordance with these findings, ^{11}C-4DST and ^{11}C-MET may be more useful for evaluating MM lesions in peripheral long bones than ^{18}F-FDG. Furthermore, Nakamoto et al. reported that ^{11}C-MET provided clearer positive findings in some patients, compared with ^{18}F-FDG. Therefore, ^{11}C-MET was considered to be useful for determining the therapeutic strategy, especially when the ^{18}F-FDG findings were equivocal or indeterminate [23]. Thus, ^{11}C-4DST and ^{11}C-MET seem to be more useful for assessing the disease activities of lytic lesions detected using CT, compared with ^{18}F-FDG. Furthermore, all the negative lesions were observed as such using ^{11}C-4DST, ^{11}C-MET, and ^{18}F-FDG.

In the second study, we demonstrated that ^{11}C-4DST and ^{11}C-MET had higher diagnostic accuracies than ^{18}F-FDG. An iliac crest biopsy is the standard method for determining bone marrow infiltration by plasma cells [26]. In smoldering MM (SMM), bone marrow biopsies reveal a 10–30 % diffuse infiltration of plasma cells, while the infiltration is less than 10 % in MGUS [5, 27] with no evidence of MM. Therefore, we evaluated the iliac crests in patients in whom a pathological diagnosis was obtained using ^{18}F-FDG, ^{11}C-4DST, and ^{11}C-MET. A statistical examination was difficult to perform because the number of patients was relatively small, but ^{11}C-MET and ^{11}C-4DST seemed to be more sensitive than ^{18}F-FDG in patients who had not yet received therapy.

In this study, all three PET/CT scans were negative in all three MGUS patients. In patients with MGUS, marrow plasma cells account for less than 10 %, while in myeloma, the bone marrow clonal cells account for no less than 10 % [24]. Both SMM and MGUS are typically not treated, but the prognoses differ. In MGUS, the overall risk of progression is about 1 % per year [28], and the median duration of MGUS and SMM before a diagnosis of myeloma is 81 and 23 months, respectively [29]. Therefore, it is important to distinguish SMM and MGUS.

In this study, extramedullary lesions were not evaluated. However, the ability of PET/CT to evaluate the whole body in a single procedure and the potential to detect medullary and extramedullary lesions during a single examination are important advantages over standard imaging techniques, such as MRI, CT, or radiographs [11]. Dankerl et al. reported that extramedullary MM was sensitively detected and localized using ^{11}C-MET. The evaluation of extramedullary lesions is important because these lesions are often difficult to detect but have a major impact on the prognosis. Nakamoto et al. reported a high level of ^{11}C-MET uptake in normal liver and pancreas; however, this situation is unlikely to cause false-negative findings because it is unusual to have extramedullary lesions in these organs [25].

When evaluating MM, diffuse lesions are more difficult to evaluate than focal lesions. The uptake of ^{18}F-FDG in the skeleton is caused by the activation of hematopoietic marrow, and its pattern and amount can vary with age and with the levels of marrow function, such as the level of function during recovery after chemotherapy or when subjected to the effect of granulocyte colony stimulating factor at the time of the PET/CT examination [30]. Because ^{11}C-4DST can be used to evaluate DNA synthesis [20], it can accumulate in active hematopoietic marrow. Thus, it may be difficult to distinguish diffuse MM lesions from hematopoietic marrow. A means of evaluating diffuse MM lesions should be a topic of future PET/CT studies.

A whole-body survey for active lesions is a unique advantage of PET/CT, and modern image processing techniques can minimize artifacts from metal prostheses. Thus, PET/CT has the potential to become a standard modality for the staging of MM.

^{11}C-4DST and ^{11}C-MET are better at detecting active lesions than ^{18}F-FDG. Therefore, the Durie/Salmon PLUS staging results determined using ^{11}C-4DST and ^{11}C-MET may differ from those determined using ^{18}F-FDG. However, the validation of a new staging method requires prognostic observation over a long observation period. The question of which tracer is the best for evaluating the viability of MM will require further observation. We are planning to evaluate this matter in a separate study.

Conclusion

^{11}C-4DST and ^{11}C-MET are useful for detecting bone marrow involvement in patients with MM, especially at an early stage, in a manner that is more clearly and more accurately than that using ^{18}F-FDG.

Acknowledgments We thank Masashi Kameyama, Takashi Sato, Shingo Kawaguchi, Takuya Mitsumoto, Fumio Sunaoka, Takaaki Kaneko, Yoshiaki Taguchi, Hiromi Suzuki, Kazuhiko Nakajima, and Kahori Miyake for their excellent technical support. This work was supported by Grants 21 A 126, 24 A 203, 25 A 204 and 26 A 116 from the National Center for Global Health and Medicine (to KK) and Grants-in-Aid for Young Scientists (B) No. 24791362 (to RM) and for Scientific Research (B) No. 22390241 (to JT) and for Scientific Research (C) No. 26461874 (to KK) from the Japan Society for the Promotion of Science.

Conflict of interest No other potential conflicts of interest relevant to this article are present.

References

1. Munshi NC, Anderson KC. Plasma cell neoplasms. In: DeVita VT, Hellman S, Rosenberg SA, editors. Cancer: principles and practice of oncology. 7th ed. Philadelphia: Lippincott Williams & Wilkins; 2005. p. 2155–88.
2. Sirohi B, Powles R. Multiple myeloma. Lancet. 2004;363:875–87.
3. Blade J, Kyle RA, Greipp PR. Multiple myeloma in patients younger than 30 years: report of 10 cases and review of the literature. Arch Intern Med. 1996;156:1463–8.
4. Kyle AR, Rajkumar SV. Multiple myeloma. N Engl J Med. 2004;351:1860–73.
5. Palumbo A, Anderson K. Multiple myeloma. N Engl J Med. 2011;364:1046–60. doi:10.1056/NEJMra1011442.
6. Rajkumar SV, Larson D, Kyle RA. Diagnosis of smoldering multiple myeloma. N Engl J Med. 2011;365:474–5. doi:10.1056/NEJMc1106428.
7. Durie BG. The role of anatomic and functional staging in myeloma: description of Durie/Salmon plus staging system. Eur J Cancer. 2006;42:1539–43.
8. Juweid ME, Cheson BD. Role of positron emission tomography in lymphoma. J Clin Oncol. 2005;23:4577–80.
9. Even-Sapir E. Imaging of malignant bone involvement by morphologic, scintigraphic and hybrid modalities. J Nucl Med. 2005;46:1356–67.
10. Caldarella C, Treglia G, Isgrò MA, Treglia I, Giordano A. The role of fluorine-18-fluorodeoxyglucose positron emission tomography in evaluating the response to treatment in patients with multiple myeloma. Int J Mol Imaging. 2012;2012:175803. doi:10.1155/2012/175803 (Epub 2012 Aug 10).
11. Bredella MA, Steinbach L, Caputo G, Segall G, Hawkins R. Value of FDG PET in the assessment of patients with multiple myeloma. AJR Am J Roentgenol. 2005;184:1199–204.
12. Derlin T, Weber C, Habermann CR, Herrmann J, Wisotzki C, Ayuk F, et al. ^{18}F-FDG PET/CT for detection and localization of residual or recurrent disease in patients with multiple myeloma after stem cell transplantation. Eur J Nucl Med Mol Imaging. 2012;39:493–500.
13. Mahfouz T, Miceli MH, Saghafifar F, Stroud S, Jones-Jackson L, Walker R, et al. ^{18}F-fluorodeoxyglucose positron emission tomography contributes to the diagnosis and management of infections in patients with multiple myeloma: a study of 165 infectious episodes. J Clin Oncol. 2005;23:7857–63.
14. Sood A, Revannasiddaiah S, Kumar R. Nuclear medicine in myeloma: the state of the science and emerging trends. Hell J Nucl Med. 2011;14:2–5.
15. Nishizawa M, Nakamoto Y, Suga T, Kitano T, Ishikawa T, Yamashita K. ^{11}C-Methionine PET/CT for multiple myeloma. Int J Hematol. 2010;91:733–4.
16. Dankerl A, Liebisch P, Glatting G, Friesen C, Blumstein NM, Kocot D, et al. Multiple myeloma: molecular imaging with ^{11}C-methionine PET/CT—initial experience. Radiology. 2007;242:498–508.
17. Muzi M, Vesselle H, Grierson JR, Mankoff DA, Schmidt RA, Peterson L, et al. Kinetic analysis of 3′-deoxy-3′-fluorothymidine PET studies: validation studies in patients with lung cancer. J Nucl Med. 2005;46:274–86.
18. Toyohara J, Okada M, Toramatsu C, Suzuki K, Irie T. Feasibility studies of 4′-[methyl-^{11}C]thiothymidine as a tumor proliferation imaging agent in mice. Nucl Med Biol. 2008;35:67–74.
19. Toyohara J, Nariai T, Sakata M, Oda K, Ishii K, Kawabe T, et al. Whole-body distribution and brain tumor imaging with ^{11}C-4DST: a pilot study. J Nucl Med. 2011;52:1322–8.
20. Minamimoto R, Toyohara J, Seike A, Ito H, Endo H, Morooka M, et al. 4′-[Methyl-^{11}C]-thiothymidine PET/CT for proliferation imaging in non-small cell lung cancer. J Nucl Med. 2012;53:199–206.
21. Morooka M, Kubota K, Kadowaki H, Ito K, Okazaki O, Kashida M, et al. ^{11}C-Methionine PET of acute myocardial Infarction. J Nucl Med. 2009;50:1283–7.
22. Bailey Dale L, Townsend David W, Valk Peter E, Maisey Michael N. Positron emission tomography. London: Springer; 2006.
23. Nakamoto Y, Kurihara K, Nishizawa M, Yamashita K, Nakatani K, Kondo T, et al. Clinical value of ^{11}C-methionine PET/CT in patients with plasma cell malignancy: comparison with ^{18}F-FDG PET/CT. Eur J Nucl Med Mol Imaging. 2013;40:708–15.
24. International Myeloma Working Group. Criteria for the classification of monoclonal gammopathies, multiple myeloma and related disorders: a report of the International Myeloma Working Group. Br J Haematol. 2003;121:749–57.
25. Dimopoulos M, Terpos E, Comenzo RL, Tosi P, Beksac M, Sezer O, et al. IMWG. International myeloma working group consensus statement and guidelines regarding the current role of imaging techniques in the diagnosis and monitoring of multiple myeloma. Leukemia. 2009;23:1545–56.
26. Schirrmeister H, Buck AK, Bergmann L, Reske SN, Bommer M. Positron emission tomography (PET) for staging of solitary plasmacytoma. Cancer Biother Radiopharm. 2003;18:841–5.
27. Walker RC, Brown TL, Jones-Jackson LB, De Blanche L, Bartel T. Imaging of multiple myeloma and related plasma cell dyscrasias. J Nucl Med. 2012;53:1091–101.
28. Kyle RA, Therneau TM, Rajkumar SV, Offord JR, Larson DR, Plevak MF, et al. A long-term study of prognosis in monoclonal gammopathy of undetermined significance. N Engl J Med. 2002;346:564–9.
29. Kyle RA, Gertz MA, Witzig TE, Lust JA, Lacy MQ, Dispenzieri A, et al. Review of 1027 patients with newly diagnosed multiple myeloma. Mayo Clin Proc. 2003;78:21–33.
30. Shreve PD, Anzai Y, Wahl RL. Pitfalls in oncologic diagnosis with FDG PET imaging: physiologic and benign variants. Radiographics. 1999;19:61–77.